Neutral and charged boron-doped fullerenes for CO$_2$ adsorption

Suchitra W. de Silva, Aijun Du, Wijitha Senadeera and Yuantong Gu[*]

Full Research Paper

Open Access

Address:
School of Chemistry, Physics and Mechanical Engineering,
Queensland University of Technology, Brisbane 4001, Australia

Email:
Yuantong Gu[*] - yuantong.gu@qut.edu.au

* Corresponding author

Abstract

Recently, the capture and storage of CO$_2$ have attracted research interest as a strategy to reduce the global emissions of greenhouse gases. It is crucial to find suitable materials to achieve an efficient CO$_2$ capture. Here we report our study of CO$_2$ adsorption on boron-doped C$_{60}$ fullerene in the neutral state and in the $1e^-$-charged state. We use first principle density functional calculations to simulate the CO$_2$ adsorption. The results show that CO$_2$ can form weak interactions with the BC$_{59}$ cage in its neutral state and the interactions can be enhanced significantly by introducing an extra electron to the system.

Introduction

The continuous dependence on fossil fuel combustion for the generation of energy has dramatically increased the atmospheric CO$_2$ concentrations over the last century. Despite concerns for global climatic changes and many attempts to sustainably generate energy, fossil fuel combustion continues to be the main source of electricity while releasing 13 Gt of CO$_2$ [1] to the atmosphere each year. Therefore CO$_2$ capture and storage (CCS) technology is a promising solution to reduce atmospheric CO$_2$ emissions [2]. Solvent absorption that is based on amines is the most common technology for the capture of CO$_2$. However this method is criticized for its very high energy consumption and operational limitations such as corrosion, slow

uptake rates, foaming and large equipment. Hence there is a huge interest in solid adsorbent materials for CCS [3-6]. In past few years metal organic frameworks (MOFs) have emerged as solid CO$_2$ adsorbent materials due to their tuneable chemical and physical properties.

Particularly, there is growing interest for metal free carbon-based nanomaterials for gas adsorption. Carbon-based nanomaterials such as fullerene, carbon nanotubes and graphene offer excellent thermal and chemical stability as CO$_2$ adsorbents [7,8]. Heterofullerenes are fullerene structures in which one or more cage carbon atoms are substituted by heteroatoms [9]. In

addition to the properties mentioned above, which are inherent to carbon-based nanomaterials, heterofullerenes also offer excellent tuneable chemical and physical properties [10]. Gas adsorption on heterofullerenes is an appealing subject. B. Gao et al. [11] studied CO_2 adsorption on calcium decorated C_{60} fullerene and F. Gao et al. [12] studied O_2 adsorption on nitrogen-doped fullerene.

Boron-doped C_{60} fullerenes are one of the most structurally stable heterofullerenes [9]. Guo et al. synthesized B-doped C_{60} fullerenes for the first time, in microscopic amounts by laser vaporisation [13]. Zou et al. [14] demonstrated the synthesis of B-doped C_{60} fullerene by using radio frequency plasma-assisted vapour deposition. Recently Dunk et al. [15] introduced a method to produce BC_{59} directly from exposing C_{60} fullerene to boron vapour. Wang et al. [16] stated that substituting a single C atom of the C_{60} fullerene with a B atom does not cause a significant distortion in the cage structure. The net change in the dihedral angle due to the doping is only 1.6% and Kurita et al. [17] predicted that due to the similarity between the C–B bond and the C–C bond, the changes in the bond lengths are less than 5%. Therefore the BC_{59} fullerene has a similar structural and thermal stability as C_{60} fullerene. Despite the numerous study results, which confirm the structural stability of B-doped C_{60} fullerene, very little studies have been done on applications of B-doped fullerene. Here, for the first time we report a study about the CO_2 adsorption on B-doped C_{60} fullerene, in which a single C atom is replaced with a B atom.

Sun et al. [8] predicted an enhanced CO_2 adsorption on $1e^-$- and $2e^-$-charged boron nitride sheets and nanotubes, which show very little chemical affinity towards CO_2 in their neutral state. Also Sun et al. [18] showed that chemical interactions between boron–carbon nanotubes (B_2CNT) and CO_2 can be enhanced by introducing extra electrons to the system. The enhanced interaction of CO_2 with adsorbent materials by electron injection has been further proved by Jiao et al. [19]. Therefore, we will investigate the CO_2 adsorption on BC_{59} fullerene in both the neutral and the $1e^-$-charged states.

Computational Details

First-principles density functional theory (DFT) calculations were carried out to study CO_2 adsorption on the BC_{59} cage. The BC_{59} structure was fully optimized in the given symmetry. The calculations were carried out at B3LYP [20-22] level of theory while using the split valence polarized basis set 6-31G(d). B97d [23,24] with the same basis set was used for calculations when non-covalent interactions are predominant. The CO_2 adsorption on BC_{59} was studied in the neutral state and in the $1e^-$-charged state. The electron distribution and transfer were analysed with Mulliken population analysis method [25].

The adsorption energies were calculated using the following equation.

$$E_{ads} = E_{CO_2/BC_{59}} - \left(E_{BC_{59}} + E_{CO_2} \right), \qquad (1)$$

where E_{ads} is the adsorption energy, $E_{CO_2 BC_{59}}$ is the total energy of the BC_{59} cage with a CO_2 molecule adsorbed and $E_{BC_{59}}$ and E_{CO_2} are the energies of the isolated BC_{59} cage and CO_2 molecule, respectively. For a favourable adsorption the calculated adsorption energy should have a negative value. To provide more accurate results for the chemisorption energy the counterpoise corrected energy [26,27] was also calculated.

The transition state was located by using the synchronous transit-guided quasi-Newton (STQN) method [28,29], which was then fully optimized by using the Berny algorithm at the B3LYP/6-31G(d) level. The optimized transition structure was used for IRC calculations at the same level of theory [30,31]. All calculations were carried out by using the Gaussian 09 package [32]. The GaussView 5 package [33] was used to visualize the optimized molecular structures, molecular orbitals and charge distributions.

Results and Discussion

The substitution of a C atom in the C_{60} fullerene by a B atom causes a charge transfer between C and B atoms, which results in an unbalanced charge distribution in the fullerene cage. The unbalanced charge distribution forms B–C complex sites for the adsorption of CO_2 (Figure 1). Here we considered two possible sites for the CO_2 adsorption: the B–C atomic site between two hexagonal rings (HH B–C site) and two identical B–C sites between a hexagonal ring and pentagonal ring (HP B–C site).

Adsorption of CO_2 on uncharged BC_{59} fullerenes

According to our simulation results, the CO_2 molecules can only form weak interactions with BC_{59} cage in its neutral state. The physisorption energy is a weak −2.04 kcal/mol (−4.1 kcal/mol for B97D/6-31G(d) calculations) and the weak interactions are mainly van der Waals interactions between the CO_2 molecule and the adsorbent. The CO_2 physisorbed configuration is shown in Figure 2. The CO_2 molecule sits parallel to the boron–carbon plane of the BC_{59} fullerene cage. The B⋯O and C⋯O bond distances are 3.25 Å and 3.71 Å, respectively. The CO_2 molecule undergoes very slight structural changes upon physisorption on the uncharged BC_{59} fullerene cage. The O–C–O angle is slightly bent to 179.7° and the changes to the C=O bond lengths are negligibly small. The doped fullerene cage hardly undergoes any structural change. The charge transfer between CO_2 and BC_{59} is only $0.008e$.
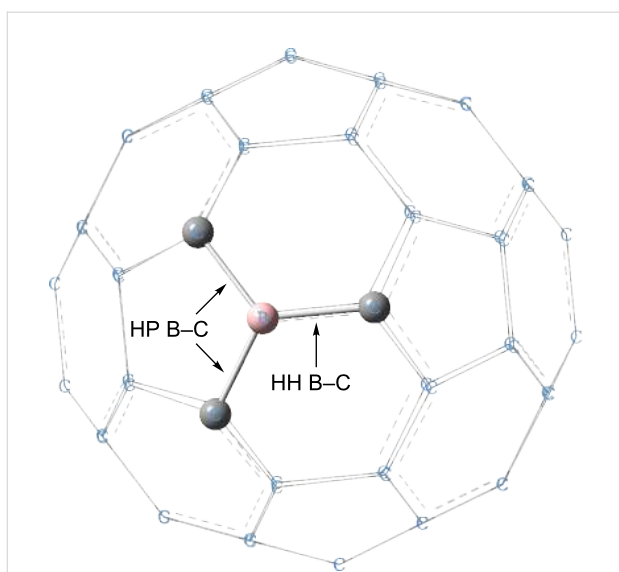
Figure 1: Sites for CO_2 adsorption on BC_{59}. The B and C atoms of HH B–C and HP B–C sites are represented as 'ball and bond'-type and the rest of the atoms are represented as 'wireframes'. Atom colour code: grey, carbon; pink, boron.
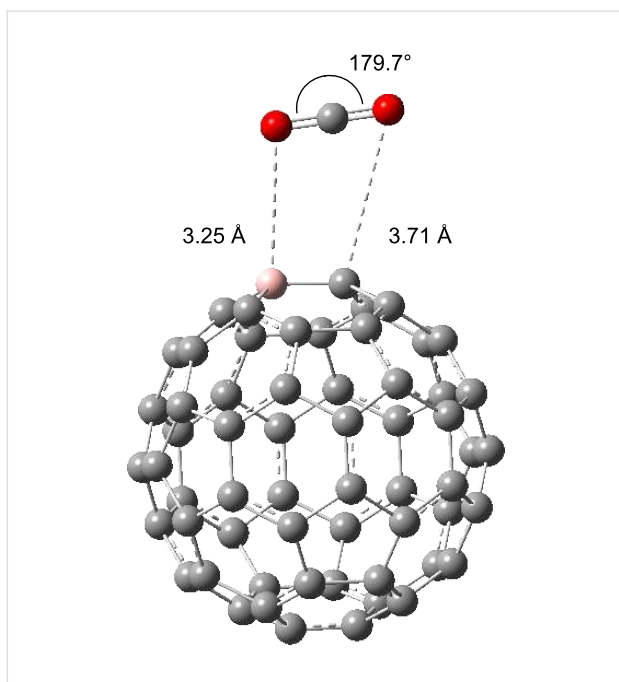

Figure 2: Configuration of physisorbed CO_2 on neutral BC_{59}. Atom colour code: grey, carbon; pink, boron; red, oxygen.

Effects of charges on the structure

Kim et al. [34] predicted that $C_{59}B^-$ should be a stable entity because of the isoelectronic configuration with C_{60}. This claim is further validated by experimental observations by Dunk et al. [15]. The Mulliken charge analysis and the electron density distributions of the lowest unoccupied molecular orbitals

(LUMO) are adopted to assess the influence of changing the charge state of BC_{59}. Figure 3 shows that the LUMO of the neutral BC_{59} is noticeably concentrated on the B atom and the neighbouring C atoms. Furthermore experimental results of Guo et al. [13] showed that boron doping creates an electron defficient site at the B atom. This suggests that an additional electron added to the system will be accepted by the B atom. This hypothesis is consistent with theoretical predictions of Kurita et al. [17] and Xie et al. [35], who stated that the doped B atom in C_{60} fullerene acts as an electron acceptor. The comparison of the Mulliken population analysis of the neutral and the $1e^-$-state of BC_{59} proves that the negative charge introduced to the system is essentially accepted by the B atom. The Mulliken atomic charge of the B atom in the BC_{59} structure in the neutral state has changed from 0.138 to 0.012 upon the introduction of the negative charge, while as shown in Figure 4 the charges on the C atoms are not changed significantly.
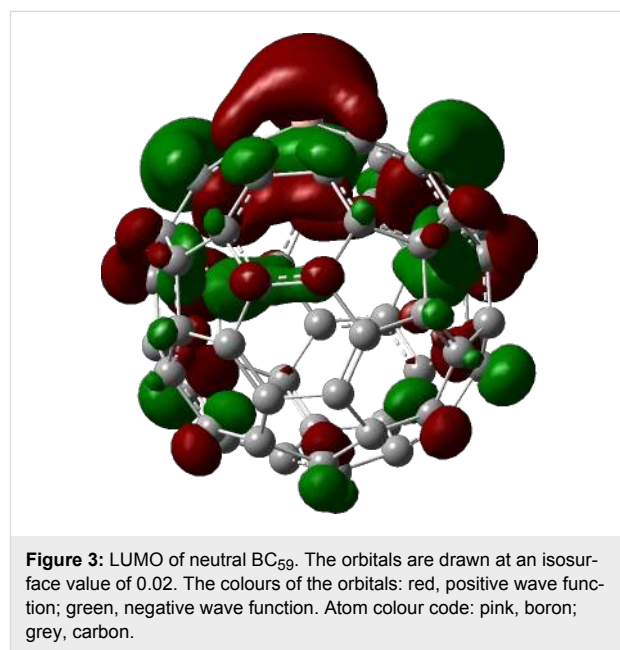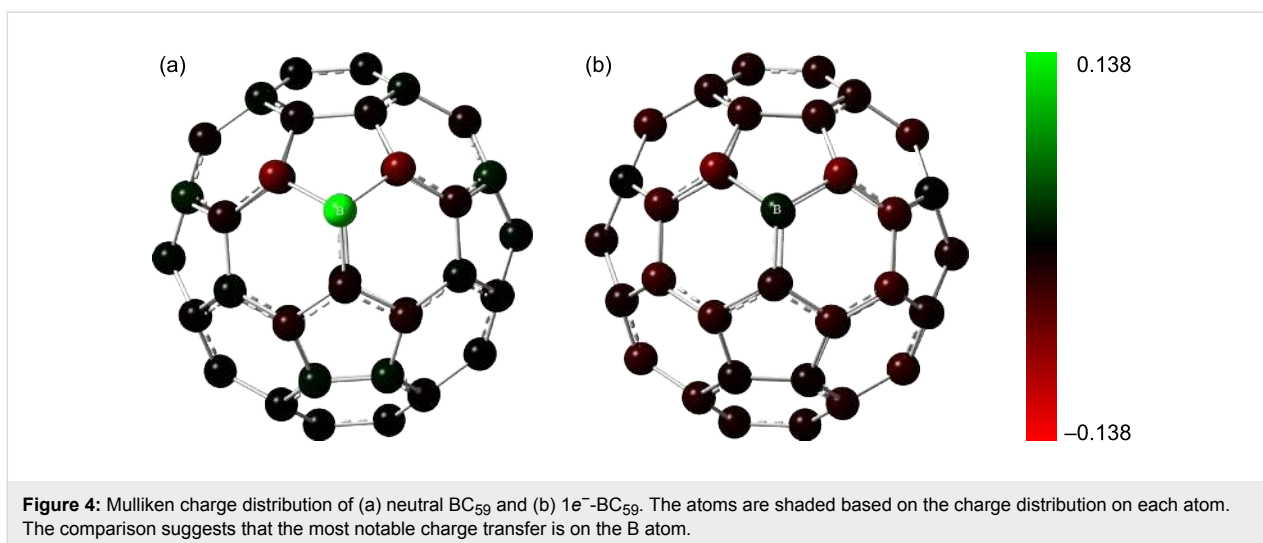

Figure 3: LUMO of neutral BC_{59}. The orbitals are drawn at an isosurface value of 0.02. The colours of the orbitals: red, positive wave function; green, negative wave function. Atom colour code: pink, boron; grey, carbon.

CO_2 adsorption on BC_{59} fullerene in the $1e^-$-state

Next we studied the CO_2 adsorption on a $1e^-$-charged BC_{59} cage. The results confirm that the negatively charged BC_{59} fullerene exhibits a stronger interaction with CO_2. Unlike the neutral BC_{59}, for which the interaction with CO_2 molecule was only physical, here the charged BC_{59} forms a substantial chemical interaction with CO_2 causing the molecule to undergo significant structural deformations. A stable CO_2 adsorption is observed at the HH B–C site. The chemisorption energy of −15.41 kcal/mol (−64.48 kJ/mol) (−13.48 kcal/mol with BSSE correction) agrees well with the ideal range of chemisorption energy (40–80 kJ/mol) for a good CO_2 adsorbent [36].
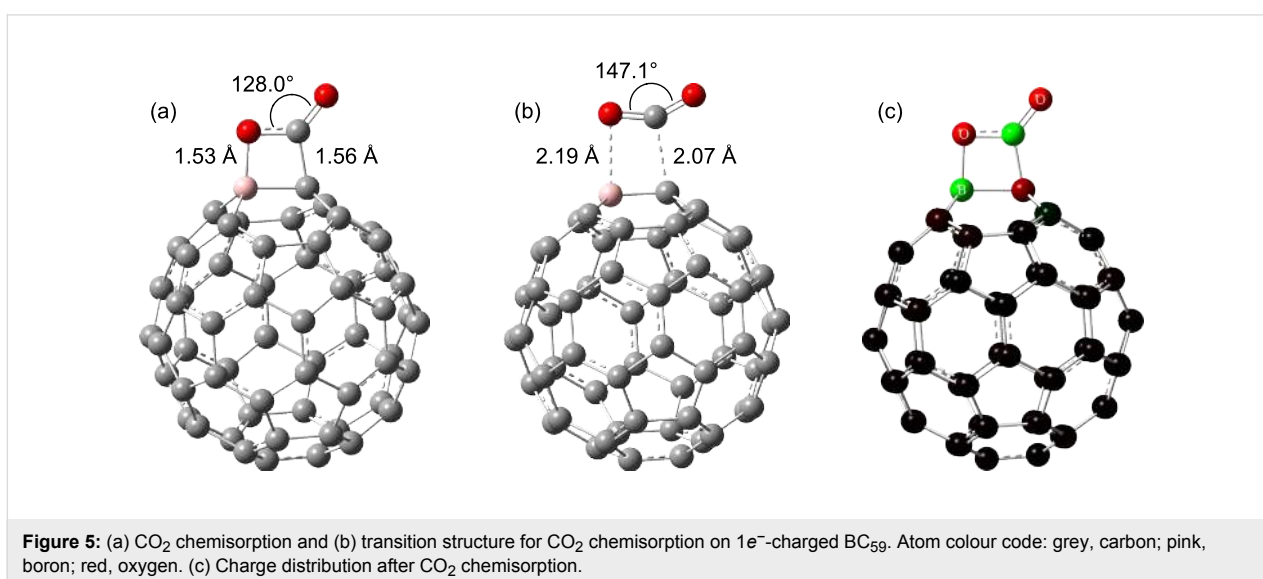
Figure 4: Mulliken charge distribution of (a) neutral BC_{59} and (b) $1e^-$-BC_{59}. The atoms are shaded based on the charge distribution on each atom. The comparison suggests that the most notable charge transfer is on the B atom.

The CO_2 molecule undergoes considerable distortion upon chemically adsorbing on the $1e^-$-charged BC_{59} fullerene. A C=O bond of the CO_2 molecule is broken when one oxygen atom forms a bond with the boron atom (which will be referred as O_a in the following discussion and the other oxygen atom as O_b) and the C atom of the CO_2 molecule forms a bond with the C atom on the HH B–C site of the cage structure. The linear O–C–O bond of CO_2 is bent to 128.0° in the adsorbed form. The C=O_b bond which is originally 1.169 Å (experimentally 1.162 Å [37]) is elongated to 1.208 Å, while the length of the C–O_a bond is expanded to 1.336 Å. The adsorption site of the BC_{59} fullerene also undergoes considerable stretching. The HH B–C site is protruded outwards by about 0.05 Å. The B–C bond of the HH B–C site has stretched from 1.496 to 1.672 Å. The Mulliken population analysis shows that a charge transfer of 0.42 has occurred from the BC_{59} fullerene to the CO_2 molecule.

Comparison of the charge distribution on BC_{59}^- before (Figure 4b) and after (Figure 5c) CO_2 adsorption, confirms that the injected electron is occupied by the CO_2 molecule.

The higher adsorption energy and the significant distortions in the structure confirm a stronger interaction between CO_2 molecule and negatively charged BC_{59} than its neutral state. These interactions can be explained due to the Lewis acidity of CO_2, which prefers to accept electrons [18]. On the other hand the B atom of the BC_{59} becomes less positively charged upon the addition of an extra electron. Therefore it becomes more likely to donate electrons to the CO_2 molecule leading to stronger interactions between the two molecules.

Figure 6 shows the minimum energy pathway for the adsorption from the physisorbed state to the chemisorbed configur-

Figure 5: (a) CO_2 chemisorption and (b) transition structure for CO_2 chemisorption on $1e^-$-charged BC_{59}. Atom colour code: grey, carbon; pink, boron; red, oxygen. (c) Charge distribution after CO_2 chemisorption.

ation. We performed frequency calculations on the optimized transition structure, which confirms that it is a first order saddle point and hence an actual transition structure. From this figure, the activation barrier for the chemisorption is estimated to be 13.25 kcal/mol (55.43 kJ/mol). The low barrier of the reaction indicates that the reaction is energetically favourable.
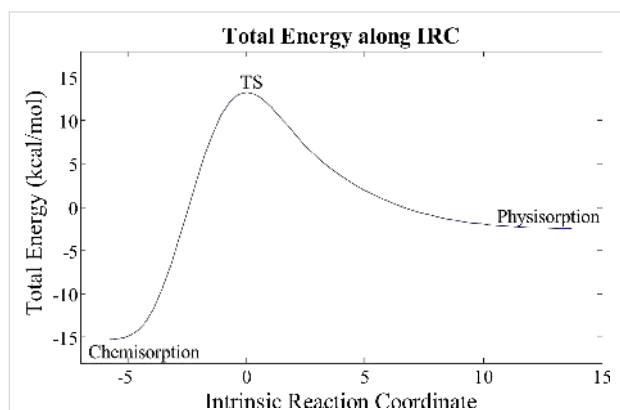

Figure 6: Intrinsic reaction pathway for CO_2 chemisorption on $1e^-$-charged BC_{59} from the physisorbed configuration. The total energy = 0 point corresponds to the total energy of $E_{CO2} + E_{BC59}{}^{-1}$.

For the desorption step, the removal of the added charge will decrease the stability of the bond between CO_2 and the doped fullerene. The thermodynamic analysis of the reaction shows that the CO_2 chemisorption is spontaneous only for temperatures less than 350 K. Therefore we suggest a method of manipulating the charge state and the temperature of the system for adsorbent recycling. Charging the system can be achieved by electrochemical methods, electrospray, and electron beam or gate voltage control methods [8].

Conclusion

By using DFT calculations we have studied the adsorption mechanisms of CO_2 on a C_{60} fullerene cage, in which a single C atom is substituted by a B atom. Our calculation results show that the BC_{59} cage, in its neutral state, shows a low chemical interaction with CO_2 molecule, which only physisorbs with $E_{ads} = -2.04$ kcal/mol. However CO_2 adsorption on the BC_{59} can be significantly enhanced by injecting negative charges into the structure. The CO_2 molecule chemisorbs on the $1e^-$-charged BC_{59} with $E_{ads} = -15.41$ kcal/mol. This study suggests that we can conclude $1e^-$-charged BC_{59} cage structure is a promising CO_2 adsorbent.

Acknowledgements

References

1. International Energy Agency, Ed. *World Energy Outlook 2011;* IEA Publications: Paris, 2011.
2. Kheshgi, H.; de Coninck, H.; Kessels, J. *Mitigation and Adaptation Strategies for Global Change* **2012,** *17,* 563–567. doi:10.1007/s11027-012-9391-5
3. Lee, K. B.; Sircar, S. *AIChE J.* **2008,** *9,* 2293–2302. doi:10.1002/aic.11531
4. Jiao, Y.; Du, A.; Zhu, Z.; Rudolph, V.; Smith, S. C. *J. Mater. Chem.* **2010,** *20,* 10426–10430. doi:10.1039/c0jm01416h
5. Jiao, Y.; Du, A.; Zhu, Z.; Rudolph, V.; Smith, S. C. *J. Phys. Chem. C* **2010,** *114,* 7846–7849. doi:10.1021/jp911419k
6. Sun, Q.; Wang, M.; Li, Z.; Du, A.; Searles, D. J. *J. Phys. Chem. C* **2014,** *118,* 2170–2177. doi:10.1021/jp407940z
7. Lee, H.; Li, J.; Zhou, G.; Duan, W.; Kim, G.; Ihm, J. *Phys. Rev. B* **2008,** *77,* 235101. doi:10.1103/PhysRevB.77.235101
8. Sun, Q.; Li, Z.; Searles, D. J.; Chen, Y.; Lu, G. (M.); Du, A. *J. Am. Chem. Soc.* **2013,** *135,* 8246–8253. doi:10.1021/ja400243r
9. Chen, Z.; King, R. B. *Chem. Rev.* **2005,** *105,* 3613–3642. doi:10.1021/cr0300892
10. Tenne, R. *Adv. Mater.* **1995,** *7,* 965–995. doi:10.1002/adma.19950071203
11. Gao, B.; Zhao, J.-x.; Cai, Q.-h.; Wang, X.-g.; Wang, X.-z. *J. Phys. Chem. A* **2011,** *115,* 9969–9976. doi:10.1021/jp2016853
12. Gao, F.; Zhao, G.-L.; Yang, S.; Spivey, J. J. *J. Am. Chem. Soc.* **2013,** *135,* 3315–3318. doi:10.1021/ja309042m
13. Guo, T.; Jin, C.; Smalley, R. E. *J. Phys. Chem.* **1991,** *95,* 4948–4950. doi:10.1021/j100166a010
14. Zou, Y. J.; Zhang, X. W.; Li, Y. L.; Wang, B.; Yan, H.; Cui, J. Z.; Liu, L. M.; Da, D. A. *J. Mater. Sci.* **2002,** *37,* 1043–1047. doi:10.1023/A:1014368418784
15. Dunk, P. W.; Rodríguez-Fortea, A.; Kaiser, N. K.; Shinohara, H.; Poblet, J. M.; Kroto, H. W. *Angew. Chem.* **2013,** *125,* 333–337. doi:10.1002/ange.201208244
16. Wang, S.-H.; Chen, F.; Fann, Y.-C.; Kashani, M.; Malaty, M.; Jansen, S. A. *J. Phys. Chem.* **1995,** *99,* 6801–6807. doi:10.1021/j100018a008
17. Kurita, N.; Kobayashi, K.; Kumahora, H.; Tago, K.; Ozawa, K. *Chem. Phys. Lett.* **1992,** *198,* 95–99. doi:10.1016/0009-2614(92)90054-Q
18. Sun, Q.; Wang, M.; Li, Z.; Ma, Y.; Du, A. *Chem. Phys. Lett.* **2013,** *575,* 59–66. doi:10.1016/j.cplett.2013.04.063
19. Jiao, Y.; Zheng, Y.; Smith, S. C.; Du, A.; Zhu, Z. *ChemSusChem* **2014,** *7,* 435–441. doi:10.1002/cssc.201300624
20. Becke, A. D. *J. Chem. Phys.* **1993,** *98,* 5648–5652. doi:10.1063/1.464913
21. Lee, C.; Yang, W.; Parr, R. G. *Phys. Rev. B* **1988,** *37,* 785–789. doi:10.1103/PhysRevB.37.785
22. Stephens, P. J.; Devlin, F. J.; Chabalowski, C. F.; Frisch, M. J. *J. Phys. Chem.* **1994,** *98,* 11623–11627. doi:10.1021/j100096a001
23. Grimme, S. *J. Comput. Chem.* **2006,** *27,* 1787–1799. doi:10.1002/jcc.20495
24. Grimme, S.; Ehrlich, S.; Goerigk, L. *J. Comput. Chem.* **2011,** *32,* 1456–1465. doi:10.1002/jcc.21759
25. Mulliken, R. S. *J. Chem. Phys.* **1955,** *23,* 1833–1840. doi:10.1063/1.1740588
26. Simon, S.; Duran, M.; Dannenberg, J. J. *J. Chem. Phys.* **1996,** *105,* 11024–11031. doi:10.1063/1.472902
27. Boys, S. F.; Bernardi, F. *Mol. Phys.* **1970,** *19,* 553–566. doi:10.1080/00268977000101561

28. Peng, C.; Schlegel, H. B. *Isr. J. Chem.* **1993,** *33,* 449–454. doi:10.1002/ijch.199300051
29. Hratchian, H. P.; Schlegel, H. B. *Finding minima, transition states, and following reaction pathways on ab initio potential energy surfaces;* Elsevier: Amsterdam, The Netherlands, 2005.
30. Peng, C.; Ayala, P. Y.; Schlegel, H. B.; Frisch, M. J. *J. Comput. Chem.* **1996,** *17,* 49–56. doi:10.1002/(SICI)1096-987X(19960115)17:1<49::AID-JCC5>3.3.CO;2 -#
31. Gonzalez, C.; Schlegel, H. B. *J. Chem. Phys.* **1989,** *90,* 2154–2161. doi:10.1063/1.456010
32. *Gaussian 09,* Revision B.01; Gaussian, Inc.: Wallingford, CT, USA, 2009.
33. *GaussView,* Version 5; Semichem Inc.: Shawnee Mission, KS, USA, 2009.
34. Kim, K.-C.; Hauke, F.; Hirsch, A.; Boyd, P. D. W.; Carter, E.; Armstrong, R. S.; Lay, P. A.; Reed, C. A. *J. Am. Chem. Soc.* **2003,** *125,* 4024–4025. doi:10.1021/ja034014r
35. Xie, R.-H.; Bryant, G. W.; Zhao, J.; Smith, V. H., Jr..; Di Carlo, A.; Pecchia, A. *Phys. Rev. Lett.* **2003,** *90,* 206602. doi:10.1103/PhysRevLett.90.206602
36. Chu, S.; Majumdar, A. *Nature* **2012,** *488,* 294–303. doi:10.1038/nature11475
37. Foresman, J. B.; Frisch, Æ. *Exploring chemistry with electronic structure methods: A Guide to Using Gaussian;* Gaussian, Inc.: Pittsburgh, PA, USA, 1996.